

Performance of Portland Cement Mortar incorporated with Reactive Magnesium Oxide

S.A. Abo-EL-ENein¹, H.A. Abdel-Gawwad^{*2}, O.A-Hodhod³, I.M.H-El-kattan⁴

¹ Faculty of science- Ain Shams University, Cairo, Egypt.

² Housing and Building National Research Center, Cairo, Egypt.

³ Faculty of Engineering – Cairo University, Giza, Egypt.

⁴ PHI for Engineering and Technology- 6th October City- Egypt.

*Hamdyabdelgawwad@yahoo.com, ibrahemelkattan86@yahoo.com

Abstract: The present paper aimed at studying the effect of reactive magnesium oxide (MgO) on the physico-mechanical properties of cement mortar (CM). Reactive magnesium oxide was prepared by calcination of hydromagnesite at 550°C, namely MgO₅₅₀. 2.5, 5, 10 and 15 wt., % MgO₅₅₀ have been added to CM. Different experimental methods such as linear expansion, water absorption, and compressive strength, were carried out to evaluate the physico-mechanical properties of CM-MgO blends. The characterization of hydration products formed a long cement matrix was done by using x-ray diffractograms (XRD), Thermogravimetric (TG/DTG) and scanning electron microscope (SEM) techniques. The results showed the CM watery consistency increased with the increase of MgO₅₅₀ content. The water absorption decreases with MgO₅₅₀ wt., % up to 5 wt., %. The addition of MgO₅₅₀ beyond 5 wt., % leads to increase the water absorption. Compressive strength enhancement was observed in case of CM having 2.5 and 5 wt., % MgO₅₅₀. The CM containing 10 and 15 wt., % MgO₅₅₀ showed the lowest compressive strength. The linear expansion of CM increases with the increase of MgO₅₅₀ content.

[S.A. Abo-EL-ENein, H.A. Abdel-Gawwad, O.A-Hodhod and I.M.H-El-kattan. **Performance of Portland Cement Mortar incorporated with Reactive Magnesium Oxide.** *J Am Sci* 2016;12(3):51-58]. ISSN 1545-1003 (print); ISSN 2375-7264 (online). <http://www.jofamericanscience.org>. 8. doi:[10.7537/marsjas12031608](https://doi.org/10.7537/marsjas12031608).

Key words: Reactive MgO, Cement mortar, Compressive strength, linear expansion, Magnesium hydroxide.

1. Introduction

Cement is obtained by pulverizing clinkers formed by calcinations of raw materials primarily consisting of lime CaO, Silicate SiO₂, Alumina Al₂O₃ and Iron Oxide Fe₂O₂. The basic raw materials used in the manufacture of Portland cement are Argillaceous and calcareous substances. Calcareous materials are Limestone, Chalk, Marine shells and argillaceous materials are Shale and Clay, Blast furnace slag. Raw materials supply the basic oxides of calcium, Silica, Alumina and Iron Oxide. The ordinary Portland cement (OPC) presents highest mechanical properties [1]-[5]. Meanwhile, it has low resistivity against acids and aggressive media [6]-[8]. There are different supplementary materials were added to improve the mechanical properties and resistivity of Portland cement to aggressive media [9]-[17]. The workability of (OPC) was enhanced using different plasticizer [18]-[20]. In this study, different experimental methods were carried out to evaluate the performance of cement mortar incorporated with reactive MgO.

2. Experimental

2.1. Materials

The materials used in this investigation were ordinary Portland cement (OPC), reactive magnesium oxide (MgO) and sand. OPC is produced by Suez Company, Suez governorate, Egypt. MgO produced by calcination of hydromagnesite (HM), which

purchased from El-Arabiya Chemical Company. Sand was supplied from El-Wasta City, Beni Suif Governorate, Egypt.

The chemical compositions of starting materials were given in Table (1). The mineralogical composition of Hydromagnesite and MgO is shown in XRD-pattern (Fig. 1). Fig. (2) shows particle distribution of OPC and HM. It is clear that the main HM particle size is 10 μm. In contrast, the mode size of OPC is 60 μm. The details of mix composition are given in Table (2).

2.2. Procedures

2.2.1. Preparation of reactive MgO

Hydromagnesite was calcined at 550 and to produce MgO, namely MgO₅₅₀. The starting calcination temperature (550°C) was chosen according to differential thermal analysis (DTA) (Fig. 3). It is shown that the endothermic peak located in the range of 60-280 °C is related to the dehydration and dihydroxylation. The carbonate is decomposed at 425-486°C (Frost et al. 2008).

2.2.2. Preparation of mortar cement mixes

The MgO was first dry-mixed with cement mortar for 2 min in a bench-top mixer to achieve homogeneity then adding mixing water. The water to cement ratio (W/C) increases with the increase of MgO₅₅₀ and MgO₁₂₅₀ content. A crater was done in the center and water was poured into the crater. The mixing operation was then completed by continuous

and vigorous mixing using ordinary gauging trowel for about three min., then cast into the cubic molds (25×25×25mm) or prism (25×25×285mm) in two layers and manually-vibrated to eliminate air voids. The samples were then covered to avoid moisture loss. After 24h of curing in 99±1 relative humidity (RH), the specimens were carefully demoulded and cured in Tap water up to 180 days.

2.2.3 Methods of investigation

The water absorption measurements were done by weighting the saturated specimens (W1) and dried specimens in oven at 80 °C for 24 hours (W2) at curing times of 3, 7, 28, 90 and 180 days. The water absorption is calculated from the following equation: Water absorption % = [(W1-W2)/ W1] x100 (ASTM C1403, 2013). Compressive strength measurements were carried out using five tones German Brūf Pressing Machine with a loading rate of 100 kg/min (ASTM C109M, 2012). The length changes of CM prisms with or without MgO₅₅₀ was determined according to ASTM C490 (2007).

2.2.4. Instrumental analyses

X-ray diffraction (XRD) was carried out on a Philips PW3050/60 X-ray diffractometer using a scanning range from 2θ of 5 to 50° with a scanning speed of 1 sec/step and resolution of 0.05°/step. Thermogravimetric analysis (TGA) was carried out by heating the sample in nitrogen atmosphere up to 1000°C with a heating rate of 20°C/min using a DT-50 Thermal Analyzer (Schimadzu Co-Kyoto, Japan). The scanning electron microphotographs were obtained with Inspect S (FEI Company, Holland) equipped with an energy dispersive X-ray analyzer (EDXA).

3. Results and Discussion

3.1. X-ray diffractograms

Figure (4) shows the X-ray-diffractograms of control cement pastes without addition of MgO₅₅₀ at 3, 28 and 180 days. The XRD patterns exhibit different crystalline peaks related to portlandites Ca(OH)₂ (CH), CSH, calcium carbonate (CC) and Ettringite (Aft). It is Obvious that, the intensity of crystalline peaks related to CH and CSH increase with time up to 180 days of curing. This is due to the continuous hydration of cement phases (C3S, C2S, C3A and C4AF). The Aft peaks are clearly observable at latter ages of hydration up to 180 days. This is related to the interaction between sulfate ions present in cement and CH, forming gypsum and in the presence of C3A, the Aft has been formed.

Figure (5) represents the X-ray diffractograms of cement pastes containing 10 wt., % MgO₅₅₀ (as addition) at 3, 28 and 180 days of hydration. It is shown that, the peak characteristics for MgO at 2θ of 42.9° are clearly observable at 3 days of curing. With the increase of curing time, the intensity of this peak

decreases and disappeared at 180 days. This confirms the consumption of MgO as results of Mg(OH)₂ and Mg-SH formation. Mg(OH)₂ and Mg-SH are difficult to be detected by XRD, due to their amorphiticity characters.

Figure (6) illustrates the X-ray diffractograms of cement pastes containing 0, 5, 10 and 15 wt., % MgO₅₅₀ (as addition) at 180 days of curing. The intensity of crystalline peak related to C3S and C2S decrease with the increase of MgO₅₅₀ content. This is due to the cationic exchange between Mg+2 and Ca+2 in these phases forming M-S-H and CH. This can be observed from the increase of the CH peak intensity with the increase of the MgO₅₅₀ content, especially in case of M5-550/A mix. The MgO peaks does not observed in case of M5-550/A and M10-550/A mixes, indicating that the MgO₅₅₀ totally consumed up to 180 days of curing. Meanwhile, this peak is observed in case of M15-550/A mix, indicating that there is unreacted MgO still retained in cement matrix.

3.2. TG/DTG-thermograms

Figure 7 (a and b) represents the TG and DTG-thermograms of control cement pastes at 3, 28 and 180 days of curing. It is obvious that, the weight loss of cement pastes increase with curing time. This is due to continuous hydration and formation of excessive hydration products content. This can be proved by the increase of CSH, CH and CC peaks intensity with time. The increase of CSH peak intensity reflects the development of compressive strength with the increase of curing time.

Figure 8 (a and b) shows the TG and DTG thermograms of M10-550/A mix at 3, 28 and 180 days of curing. The TG curves show that the weight loss of cement paste increases with curing time, suggesting, the successive hydration product formation with the time. The DTG curves exhibit four different endothermic peaks related to CSH, M-SH, Mg(OH)₂, CH and CC. The increase of Mg(OH)₂ intensity peak with the time proves the continuous hydration of MgO₅₅₀. The increase in CC peak intensity with time is mainly due to the atmospheric carbonation of MH and CH.

Figure 9 (a and b) shows the TG and DTG-thermograms of M0, M5-550/A, M10-550/A and M15-550/A at 180 days of hydration. It is clear that there is a marginal increase in weight loss of cement paste with the increase of MgO₅₅₀ addition. The DTG curves showed that, Mg(OH)₂ peaks intensity increase with the increase of MgO₅₅₀ addition. The CSH peak intensity decreases with the increase of MgO₅₅₀, especially in M10-550/A and M15-550/A mixes. This is due to the dilution of cement content.

3.3. Linear Expansion

Figure (10) represents the linear expansion of CM containing 0, 5, 10 and 15 wt., % MgO₅₅₀ up to 28

days of curing in Tapwater at $23\pm 2^\circ\text{C}$. Evidently, the linear expansion of CM increases with MgO_{550} content. This is attributed to the continuous MgO_{550} hydration.

3.4. Water absorption

Figure (11) shows the water absorption of CM containing 0 (M0), 2.5 (M2.5-550/A), 5 (M5-550/A), 10 (M10-550/A) and 15 (M15-550/A) wt., % MgO_{550} (as addition). Obviously, the water absorption values of CM containing 2.5 and 5 wt., % MgO_{550} are lower than those of control CM, suggesting the densification occurred by finely powdered MgO which fills open pores. Increasing MgO_{550} addition leads to increase the water absorption of CM up to 180 days. This may be due to the dilution of cement content, leading to the formation of little hydration products content.

3.5. Compressive strength

Figure (12) illustrate the compressive strength values of M0, M2.5-550/A, M5-550/A, M10-550/A and M15-550/A mixes. Clearly, the addition of 2.5 and 5 wt., % MgO_{550} leads to increase the compressive strength of CM. This may be explained by the densification of CM matrix caused by MgO_{550} with high fineness. A significant reduction in compressive strength was observed in case of M10-550/A and M15-550/A mixes. This should be explained by the

dilution of cement content as well as the formation of high magnesium silicate hydrate (MSH) with low binding capacity compared to calcium silicate hydrate (CSH). Moreover, the high MgO_{550} addition leads to the formation of high $\text{Mg}(\text{OH})_2$ content which acts as destructive agent for the binding capacity of CM.

3.6. SEM photographs.

Figure (13) displays the SEM-photographs of M0 and M5-550/A at 3 and 180 days as well as M10-550/A and M15-550/A at 180 days of curing. The SEM-photos exhibits different microstructures. The SEM of M0 at 3 days seems to be less compact, containing small aggregates distributing along the surface of microstructure. With time increasing, the microstructure becomes denser. This proves the continuous hydration and formation of hydrated products with time. The SEM of M5-550/A mix seems to be more compact microstructure comparing with M0 mix at 3 and 180 days. This confirms the compressive strength results. As the amount of MgO_{550} increases the amount of unreacted MgO_{550} increases, confirming the XRD results. In addition, M10-550/A and M15-550/A microstructures show the lowest compaction, confirming the fact that the increases of MgO_{550} with 10 and 15 wt., % leads to the dilution of cement content.

Table (1): Chemical compositions of OPC and hydromagnesite.

Oxide, %	SiO_2	Al_2O_3	Fe_2O_3	CaO	MgO	Na_2O	K_2O	SO_3	TiO_2	P_2O_5	L.O.I	Total
OPC	20.5	4.86	3.72	62.8	2.35	0.12	0.08	2.14	0.04	0.05	2.35	99.92
Hydromagnesite	0.09	0.08	0.01	0.4	42.95	-	0.18	0.04	-	0.03	56.19	99.94

Table (2): Mix composition of cement mortar with MgO_{550} .

Mix symbol	MgO wt. %	Cement, wt. %	Water/ Cement (W/c) ratio	Calcination temperature, $^\circ\text{C}$
M0	0	100	0.40	-
M5-550	5	100	0.40	550
M10-550	10	100	0.40	550
M15-550	15	100	0.40	550

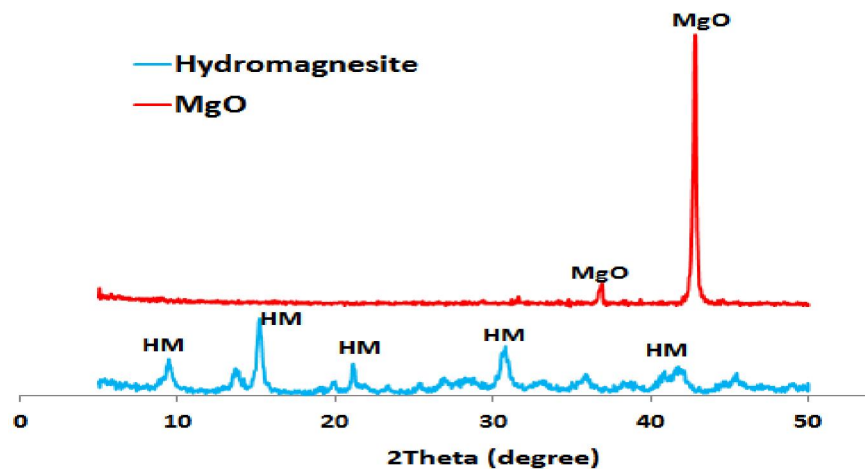


Fig. (1): XRD-pattern of hydromagnesite (MH) and MgO .

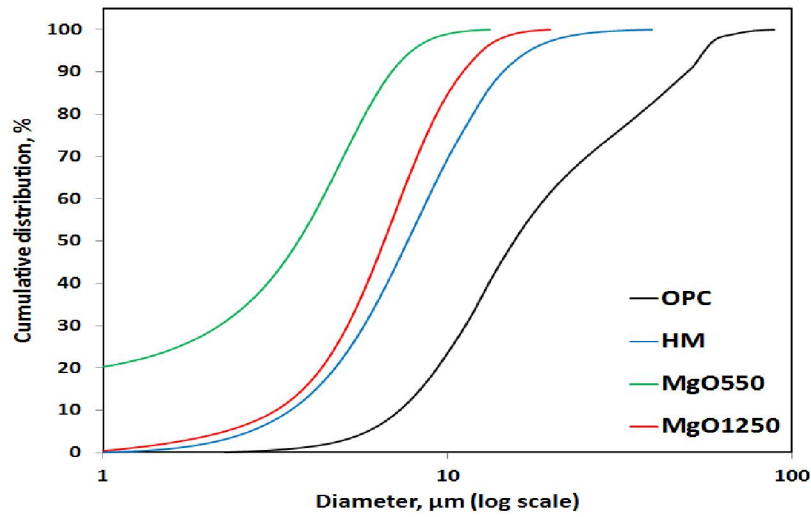


Fig. (2): Particle size distribution of OPC, HM, MgO₅₅₀ and MgO₁₂₅₀

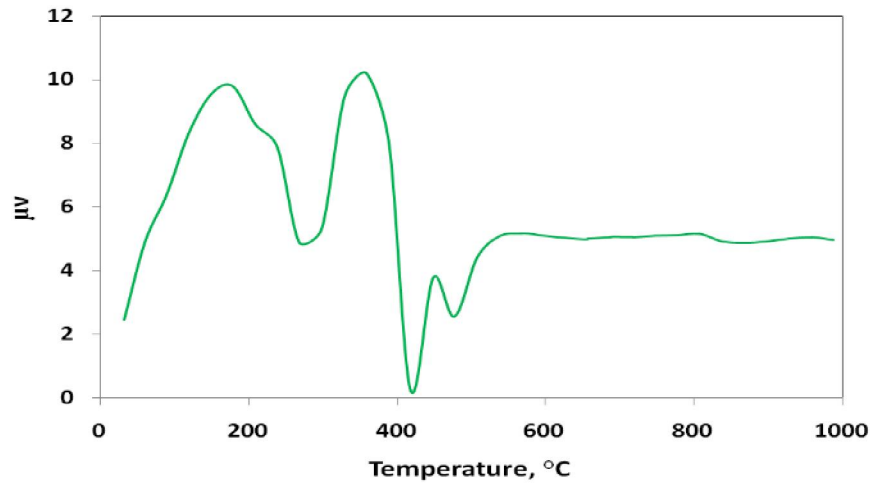


Fig. (3): DTA-thermogram of hydromagnesite (MH)

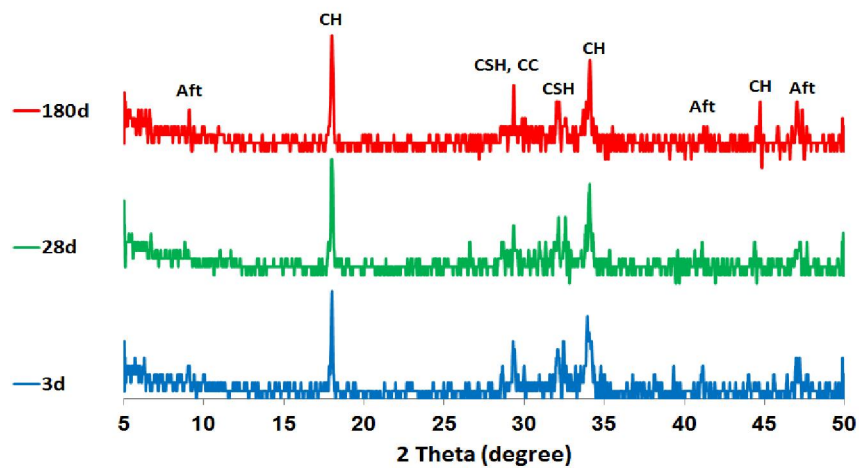


Fig. (4): XRD-patterns of cement pastes without addition of MgO₅₅₀ at 3, 28 and 180 days

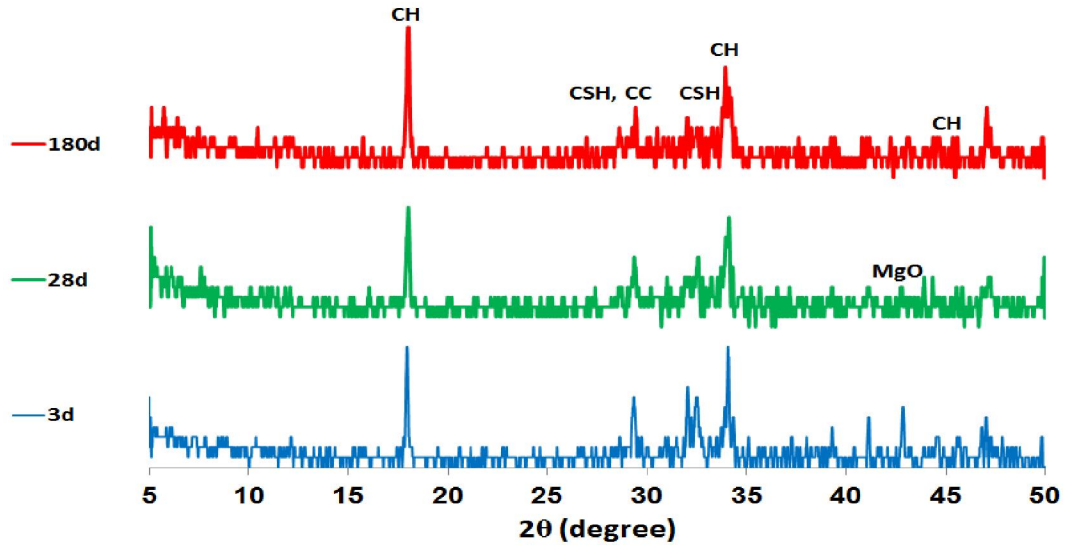


Fig. (5): XRD-patterns of cement pastes containing 10 wt., % MgO_{550} (as addition) at 3, 28 and 180 days.

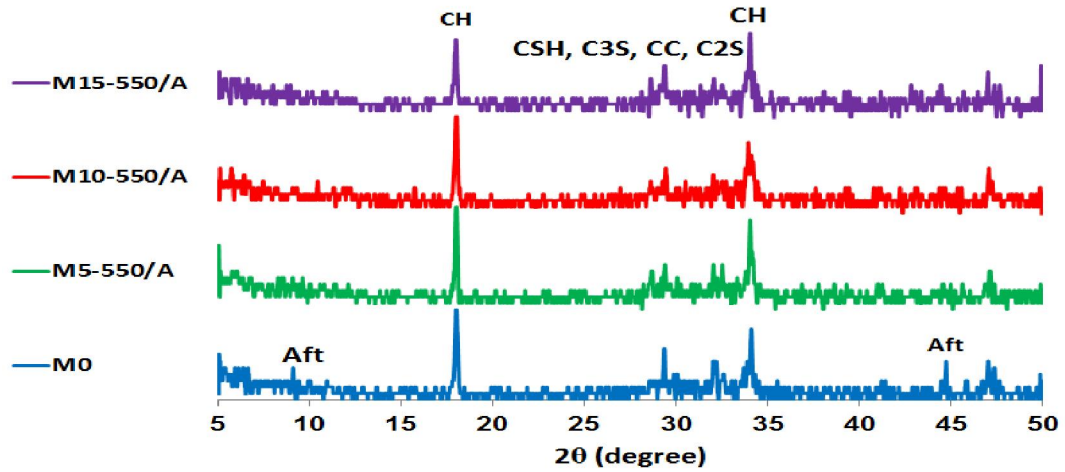


Fig. (6): XRD patterns of cement pastes containing 0, 5, 10 and 15 % wt.% MgO_{550} (as addition) at 180 days

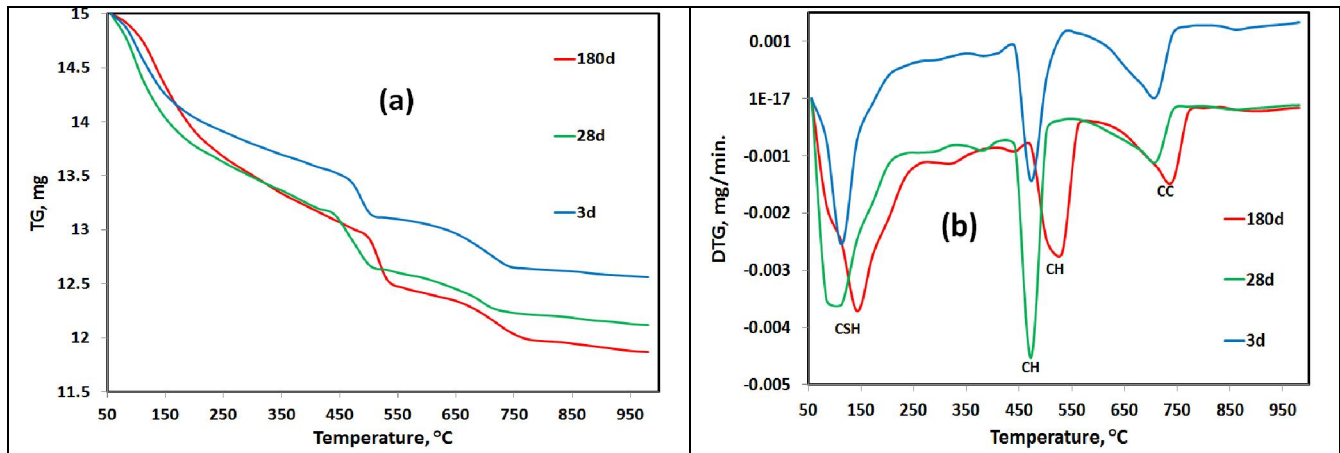


Fig. (7): (a) TG and (b) DTG-thermograms of M0 mix at 3, 28 and 180 days

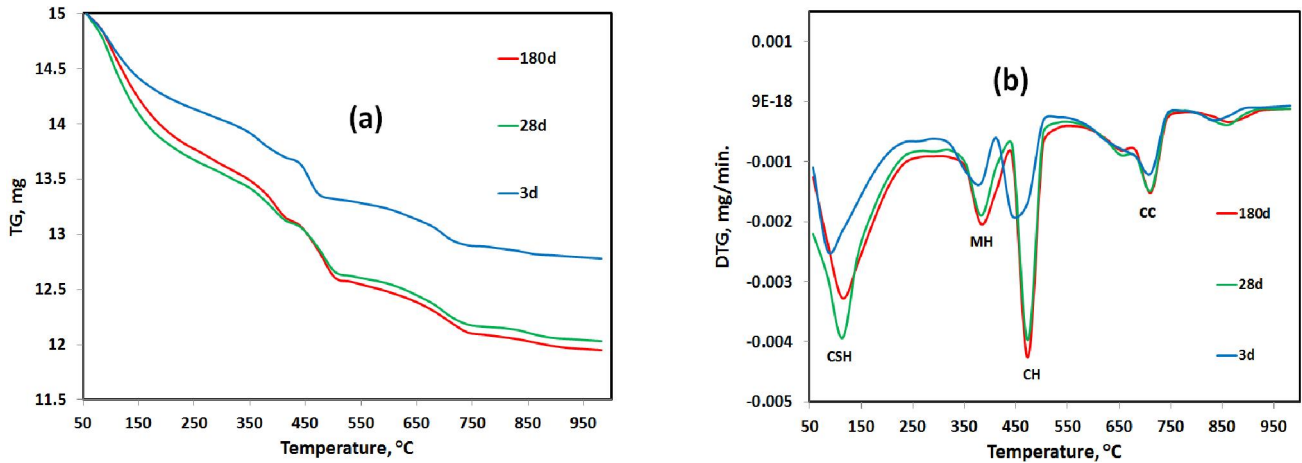


Fig. (8): (a) TG and (b) DTG-thermograms of M10-550/A at 3, 28 and 180 days

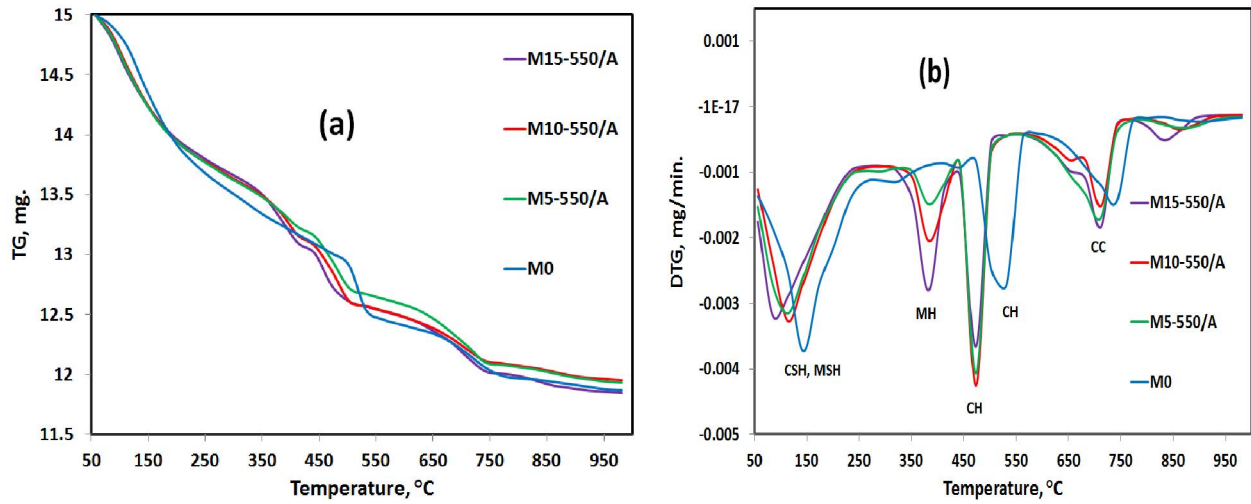


Fig. (9): (a) TG and (b) DTG-thermograms of M0, M5-550/A, M10-550/A and M15-550/A mixes at 180 days

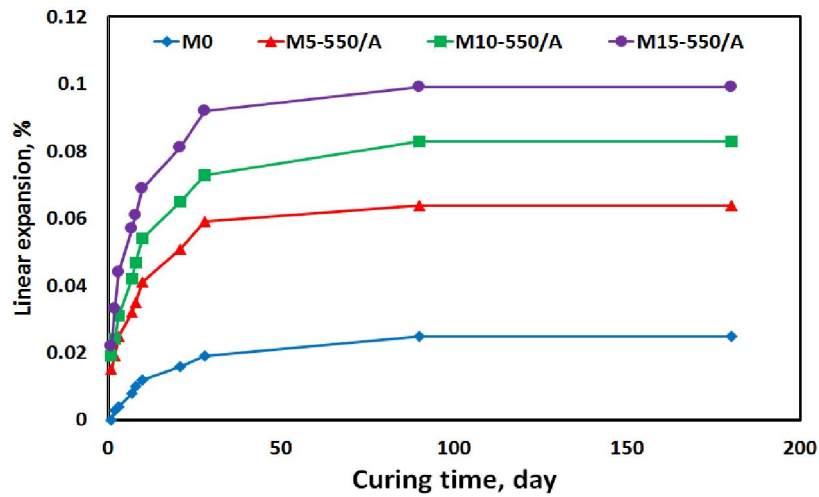


Fig. (10): Linear expansion of M0, M5-550/A, M10-550/A and M15-550/A mixes up to 28 day

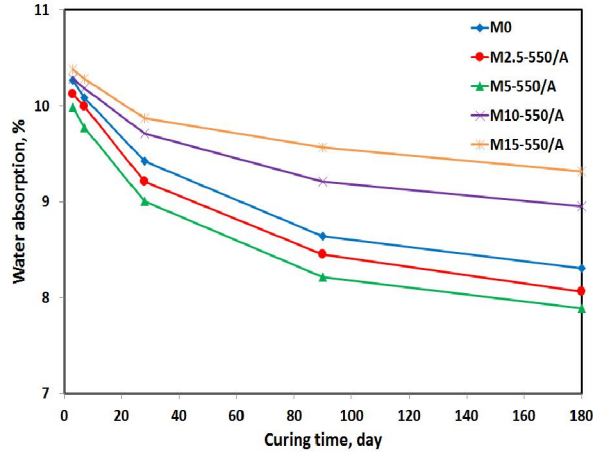


Fig. (11): Water absorption of CM with or without MgO_{550} (as addition)

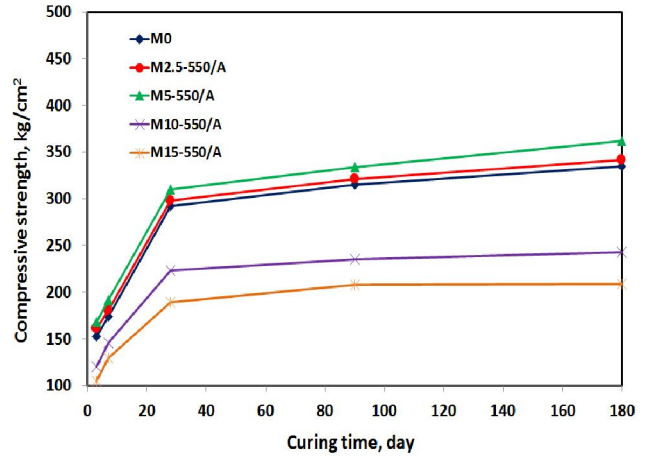


Fig. (12): Compressive strength of CM with or without MgO_{550} (as addition)

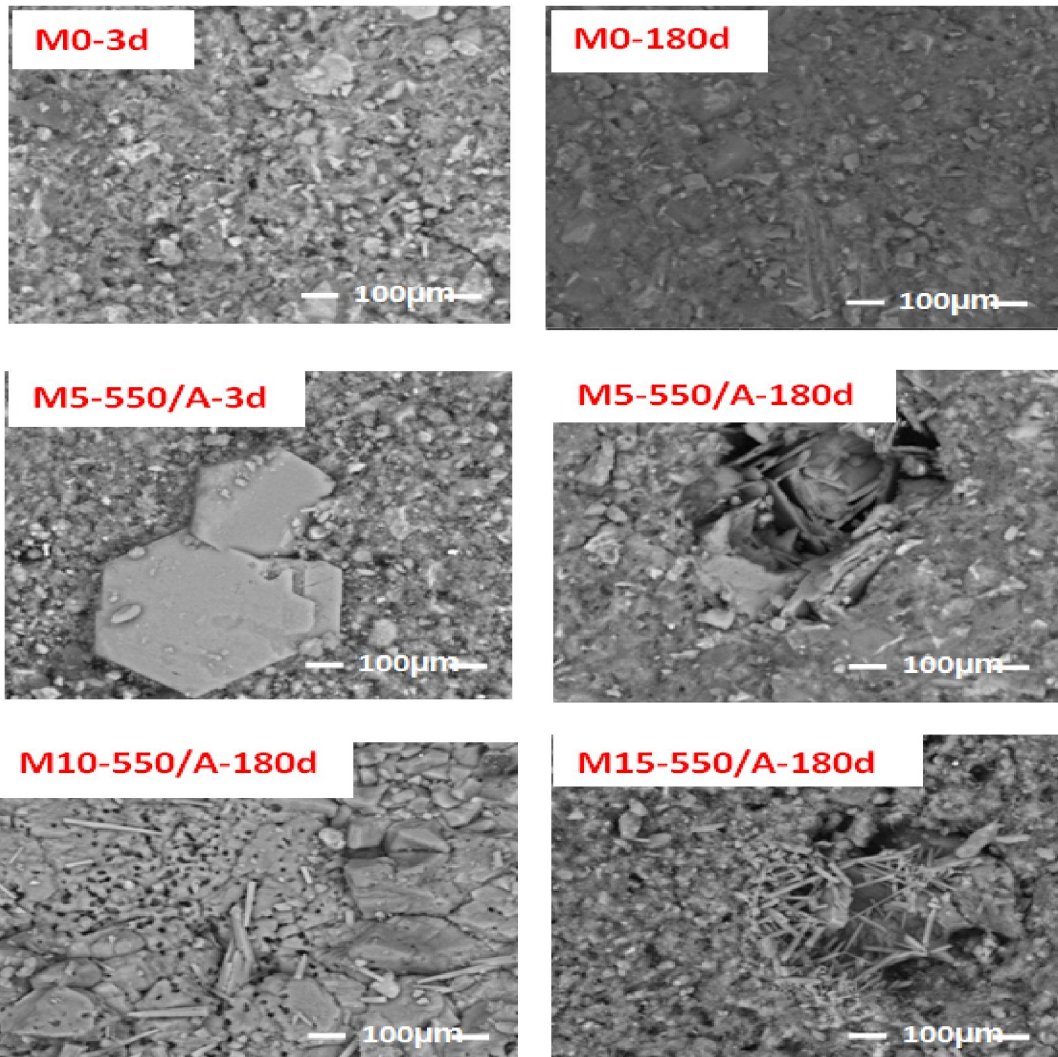


Fig. (13): SEM-photographs of M0 and M5-550/A at 3 and 180 days as well as M10-550/A and M15-550/A at 180 days

4. Conclusion

Several findings can be concluded as follows:

Compressive strength enhancement and water absorption reduction were observed in CM containing 2.5 and 5 wt., % MgO₅₅₀. The addition of MgO₅₅₀ beyond 5 wt., % leads to increase of water absorption as well as decrease compressive strength. The linear expansion of CM increase with MgO₅₅₀ content.

The XRD-patterns and TG/DTG- thermograms proved that the rate of MgO₅₅₀ hydration increase with time, forming excessive Mg(OH)₂ content. The SEM-photographs confirmed that the densification effect of MgO₅₅₀ with 2.5 and 5 wt., % which fills open pores of CM, yielding high compact microstructure.

References

1. Shaswata Mukherjee, Saroj Mandal, Adhikari. U.B," Study on the physical and mechanical property of ordinary portland cement and fly ash paste", *International Journal Of Civil And Structural Engineering* 2, (3); 2012.
2. Saleh Abd El-Aleem Mohamed, Abd El-Rahman Ragab, "Physico-Mechanical Properties and Microstructure of Blended Cement Incorporating Nano-Silica", *International Journal of Engineering Research & Technology (IJERT)*, 3, (7); 2014.
3. Valeria Corinaldesi, Alida Mazzoli, Giacomo Moriconi, "Mechanical and Physical Properties of Cement Mortars Containing Plastic Waste Particles", *international secondary conference on sustainable construction material and technology*, 2010.
4. Ewelina Tkaczewska," Mechanical Properties of Cement Mortar Containing Fine-Grained Fraction of Fly Ashes", *Open Journal of Civil Engineering*, (3); 2013, pp 54-68.
5. M. S. Morsy, S. H. Alsayed, M. Aqel, " Effect of Nano-clay on Mechanical Properties and Microstructure of Ordinary Portland Cement Mortar", *International Journal of Civil & Environmental Engineering IJCEE-IJENS*, 10, (01); 2010.
6. R.L. Sharma, S.P. Pandey," Influence of mineral additives on the hydration characteristics of ordinary Portland cement", *Cement and Concrete Research*, 29 (1999) pp 1525–1529.
7. D. Israel, D. E. Macphee, E. E. Lachowski, "Acid attack on pore-reduced cements". *Journal Of Materials Science* 32; (1997).
8. Abdoullah Namdar, Fadzil Mat Yahaya," Enhancement of Cement Mortar Mechanical Properties with Replacement of Seashell Powder, *International Journal of Civil, Environmental, Structural, Construction and Architectural Engineering* 8, (2), 2014.
9. Zongjin Li, Zhu Ding, "Property improvement of Portland cement by incorporating with metakaolin and slag", *Cement and Concrete Research*, Volume 33, November 2002.
10. V.G Papadakis, S Tsimas, " Supplementary cementing materials in concrete: Part I: efficiency and design", *Cement and Concrete Research*, Volume 32, May 2002.
11. Ş. Targana, A. Olgun, Y. Erdogan, V. Sevincc, "Effects of supplementary cementing materials on the properties of cement and concrete", *Cement and Concrete Research*, vol 32, October 2002.
12. Vagelis, G Papadakis," Effect of supplementary cementing materials on concrete resistance against carbonation and chloride ingress ", *Cement and Concrete Research*, Volume,30, February 2000.
13. H. Toutanji, N. Delatte, S. Aggoun, R. Duval, A. Danson, " Effect of supplementary cementitious materials on the compressive strength and durability of short-term cured concrete " *Cement and Concrete Research*, Volume 34, February 2004.
14. Jacek Gołaszewski, Janusz Szwabowski, "Influence of superplasticizers on rheological behaviour of fresh cement mortars", *Cement and Concrete Research*, Volume 34, February 2004.
15. Luciano Senff, João A. Labrincha, Victor M. Ferreira, Dachamir Hotza, Wellington L. Repette, "Effect of nano-silica on rheology and fresh properties of cement pastes and mortars ", *Construction and Building Materials*, Volume 23, July 2009.
16. J. Monzó, J. Payá, M.V. Borrachero, I. Girbés, "Reuse of sewage sludge ashes (SSA) in cement mixtures: the effect of SSA on the workability of cement mortars ", *Waste Management*, Volume 23, 2003.
17. M. Berra, F. Carassiti, T. Mangialardi, A.E. Paolini, M. Sebastiani," Effects of nanosilica addition on workability and compressive strength of Portland cement pastes", *Construction and Building Materials*, Volume 35, October 2012.
18. Min-Hong Zhang, Kritsada Sisomphon, Tze Siong Ng, Dao Jun Sun, "Effect of superplasticizers on workability retention and initial setting time of cement pastes, *Construction and Building Materials*, Volume 24, September 2010.
19. Irshad Masood, S.K. Agarwal, " Effect of various superplasticizers on rheological properties of cement paste and mortars", *Cement and Concrete Research*, Volume 34, November 2004.
20. G. Quercia, G. Hüsken, H.J.H. Brouwers, " Water demand of amorphous nano silica and its impact on the workability of cement paste", *Cement and Concrete Research*, Volume 42, February 2012.